Supporting Information

Krebs et al. 10.1073/pnas.0913035107

SI Methods

Plant Growth Conditions. *Arabidopsis thaliana* ecotype Col-0 seeds were grown on soil or plates containing 1× MS salt, 1% sucrose solidified with 0.5% phyto agar, and 50 μg/mL kanamycin. Plates prepared for mutants carrying an EtOH-inducible construct contained 1/10 MS medium, 0.5% sucrose, 10 mM Mes-KOH (pH 5.8) solidified with 1% phytoagar for vertical incubation and 0.2% EtOH. Agar and MS basal salt mixture were purchased from Duchefa. Seeds were surface sterilized with EtOH or bleach for growth on plates. All seeds were stratified for 48 h at 4 °C. Plants were grown at 22 °C with cycles of 16 h light and 8 h darkness.

The root length of seedlings grown on vertical plates was measured from digital photographs by using the program ImageJ 1.41 (National Institutes of Health).

Pictures of whole plants, leaves, and plates, etc., were acquired using a Power Shot G1 camera (Canon, Tokyo, Japan). Image processing was performed with Adobe Photoshop.

Plant Transformation. The binary constructs were introduced into the *Agrobacterium tumefaciens* strain GV3101:pMP90 and selected on 5 μg/mL rifampicin, 10 μg/mL gentamycin, and 100 μg/mL spectinomycin. *Arabidopsis thaliana* ecotype Col-0 wild-type or *vha-a2 vha-a3* plants were used for transformation, using standard procedures. Transgenic plants were selected on plates containing 1× MS medium with 1% sucrose and 50 μg/mL kanamycin.

Construct Design. The constructs *VHA-a1-GFP*, *VHA-a2-GFP*, and *VHA-a3-GFP* have been already described (1).

PCR, RT-PCR, and qRT-PCR. Genomic DNA was extracted at 60 °C for 1 h from leaf tissue in 425 μL of PEB [100 mM Tris-HCl (pH 8.0), 50 mM EDTA (pH 8.0), 500 mM NaCl, 0.7% SDS], precipitated with 85% isopropanol, washed with 70% EtOH, and dissolved in 200 μL of 10 mM Tris-HCl (pH 8.5).

RNA isolation and cDNA synthesis were performed as described previously (2). The presence of the *VHA-a2* transcript was tested by RT-PCR and the amplification of *ACTIN2* served as cDNA loading control. The cDNA was amplified with VHA-a2. FOR (5′-CGAATACGAGATCGGAGAC-3′) and VHA-a2.REV (5′-TGCAACTTG TCGTTATTAGCATTG-3′) for 27 cycles and with ACT2.FOR (5′-TCCAAGCTGTTCTCTCCTTG-3′) and ACT2.REV (5′-GAGGGCTGGAACAAGACTTC-3′) for 23 cycles. The transcript starting at the T-DNA insertion was amplified with TL2 (5′- CAATCAGCTGTTGCCCGTCTCAC -3′) and VHA-a2.REV for 28 cycles.

To check for the presence of the *pap1-D* T-DNA, PCR was performed on genomic DNA using a T-DNA-specific primer (5′-CATTGCCCAGCTATCTGTCAC-3′) and a primer that matches ≈700 bp downstream of the *pap1-D* T-DNA insertion (5′-GAAGCCAAGTATCAAGAGAGG-3′).

Quantitative RT-PCR (qRT-PCR) was performed in the presence of the double-stranded DNA-binding dye SYBR Green (SYBR greenER qPCR Super-Mix Universal, Invitrogen) and the reaction was monitored with the Mastercycler ep *realplex* (Eppendorf). The *pap1-D* transcript was amplified with MYB75.FOR (5′-TGTAAGAGCTGGGCTAAACCGG-3′) and MYB75.REV (5′-GTTGTCGTCGCTTCAGG AACCA-3′) and was normalized to the transcript levels of *TUBULIN BETA-2*, which was amplified with TUB2.FOR (5′-GAGCCTTACAACGCTACTCTGTCTGTC-3′) and TUB2.REV (5′-ACACCAGACATAGTAGCAGAAATCAAG-3′).

Transmission Electron Microscopy. Samples for transmission electron microscopy were prepared as described previously in (1). Immunogold labeling was performed on ultrathin thawed Tokuyasu cryosections of formaldehyde-fixed (8%, 3 h) and sucrose-infiltrated (2.1 M) root tips, using rabbit anti-GFP serum (1:25; Abcam) or rabbit anti-VHA-E serum (1:500) (1, 3) and silver-enhanced (HQ Silver, 6 min; Nanoprobes) goat (Fab′) anti-rabbit IgG coupled to Nanogold (no. 2004; Nanoprobes).

CLSM. Fluorescence microscopy was performed using the Zeiss Axiovert LSM510 Meta confocal laser-scanning microscope. The microscope was equipped with a Zeiss C-Apochromat 63× water immersion objective. For image acquisition the LSM confocal software was used. GFP was excited using the 488-nm laser line and the emission was detected between 510 and 540 nm. Post-acquisition image processing was performed using Adobe Photoshop software.

In Situ Calibration pH. In situ calibration of BCECF was performed with 5-day-old *Arabidopsis* seedlings, which were loaded with the dye as mentioned in *Methods*. Fifteen minutes before measurement the seedlings were incubated in pH equilibration buffers according to refs. 4 and 5. The buffers contained 50 mM Mes-BTP (pH 5.2–6.4) or 50 mM Hepes-BTP (pH 6.8–7.6) and 50 mM ammonium acetate. The calibration curve was obtained by plotting the average ratio values of 15 seedlings against the pH.

Measurement of Cell Sap pH. Cell sap was extracted from rosette leaves of 3- to 4-week-old plants. Leaves were chopped off and squeezed in a 1.5-mL reaction tube with a micropestle for 1 min. Samples were centrifuged for 1 min at RT at 20,000 × *g*. The supernatant was transferred into a new tube and the procedure was repeated once. Supernatants of two extractions were pooled and the pH of the solution was immediately measured using a semimicroelectrode (InLab 422; Mettler-Toledo).

1. Dettmer J, Hong-Hermesdorf A, Stierhof Y-D, Schumacher K (2006) Vacuolar H+-ATPase activity is required for endocytic and secretory trafficking in Arabidopsis. *Plant Cell* 18: 715–730.
2. Dettmer J, et al. (2005) Essential role of the V-ATPase in male gametophyte development. *Plant J* 41:117–124.
3. Betz M, Dietz K-J (1991) Immunological characterization of two dominant tonoplast polypeptides. *Plant Physiol* 97:1294–1301.
4. Yoshida S (1994) Low temperature-induced cytoplasmic acidosis in cultured mung bean (Vigna radiata [L.] Wilczek) cells. *Plant Physiol* 104:1131–1138.
5. Swanson SJ, Jones RL (1996) Gibberellic acid induces vacuolar acidification in barley aleurone. *Plant Cell* 8:2211–2221.

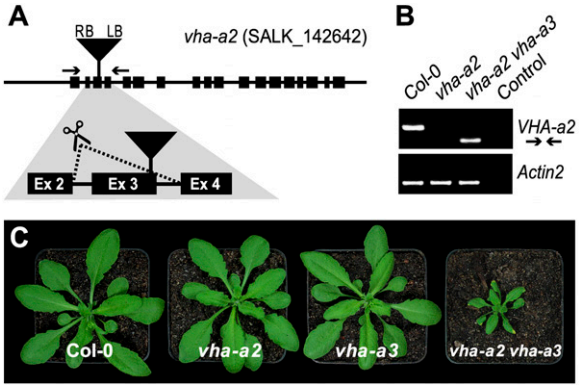

Fig. S1. *vha-a2* T-DNA insertion line. (*A*) Genomic structure of VHA-a2 (At2g21410). The SALK line 142642 carries a T-DNA insertion in the third exon of *VHA-a2*. (*B*) The absence of the transcript in *vha-a2* was confirmed by RT-PCR using a gene-specific primer pair. In *vha-a2 vha-a3* the T-DNA, exon 3, and the flanking introns are spliced out, resulting in a truncated *VHA-a2* transcript. (*C*) *vha-a2* and *vha-a3* show normal growth, whereas *vha-a2 vha-a3* is severely affected. Plants were grown under 16-h light/8-h dark cycles and pictures were taken 25 days after germination (DAG).

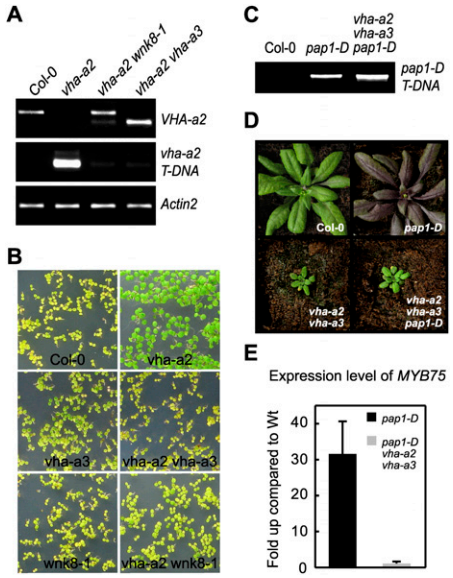

Fig. S2. T-DNA splicing and silencing in the *vha-a2* mutant background. (*A*) RT-PCR illustrating the presence or the absence of the VHA-a2 T-DNA insertion in different genetic backgrounds. For amplification either a gene-specific primer pair (*Top*) or a gene-/T-DNA-specific primer combination (*Middle*) was used. *Actin2* amplification was used as a cDNA loading control (*Bottom*). In *vha-a2 vha-a3* and in the F_2 generation of *vha-a2 wnk8-1* the T-DNA is spliced out, whereas the T-DNA transcript (*Middle*) is hardly detectable. Note that in the F_2 generation of *vha-a2 wnk8-1* the wild-type transcript (upper band) as well as the truncated transcript (lower band) is present. (*B*) Seedlings were grown for 6 days on plates containing 1× MS, 1% suc, and 50 μg/mL kanamycin. The kanamycin resistance (*nptII*) is silenced in *vha-a3*, *wnk8-1*, *vha-a2 vha-a3*, and *vha-a2 wnk8-1* but not in *vha-a2*. (*C*) PCR on genomic DNA with a gene-/T-DNA-specific primer pair, showing the presence of the *pap1-D* T-DNA insertion in different genetic backgrounds. (*D*) In the activation-tagged *pap1-D* mutant the transcription factor *MYB75* is strongly overexpressed, leading to an enhanced anthocyanin biosynthesis and accumulation. In the *vha-a2 vha-a3 pap1-D* triple mutant the *pap1-D* phenotype is lost. Pictures were taken 29 DAG. (*E*) qRT-PCR on cDNA of *pap1-D* and *vha-a2 vha-a3 pap1-D* reveals that the *MYB75* transcript is 30 times more abundant in *pap1-D* than in the wild type but not in the *vha-a2 vha-a3 pap1-D* triple mutant. Error bars show SD of three technical replicates.

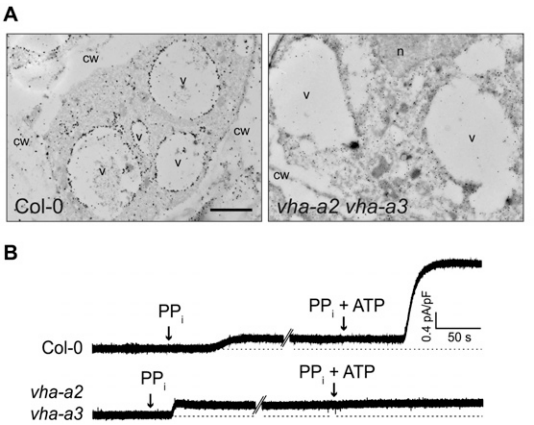

Fig. S3. *vha-a2 vha-a3* is a null mutant for the tonoplast V-ATPase. (*A*) Immunogold-labeled V_1 subcomplexes in 4- to 5-day-old *Arabidopsis* root tip cells. Electron micrographs of ultrathin cryosections were labeled with anti-VHA-E antibodies. In wild-type cells the tonoplast and the cytosol were labeled, whereas in *vha-a2 vha-a3* no labeling of the tonoplast could be observed. cw, cell wall; n, nucleus; v, vacuole. (Scale bar, 2 μm.) (*B*) PP_i- and ATP-induced H^+ currents in isolated *Arabidopsis* mesophyll vacuoles. Currents were recorded before and after application of PP_i alone or together with ATP. Arrows indicate the onset of the bath perfusion with the respective effectors. V-PPase currents could be induced in wild type and *vha-a2 vha-a3*, whereas V-ATPase currents could be observed only in wild-type vacuoles.

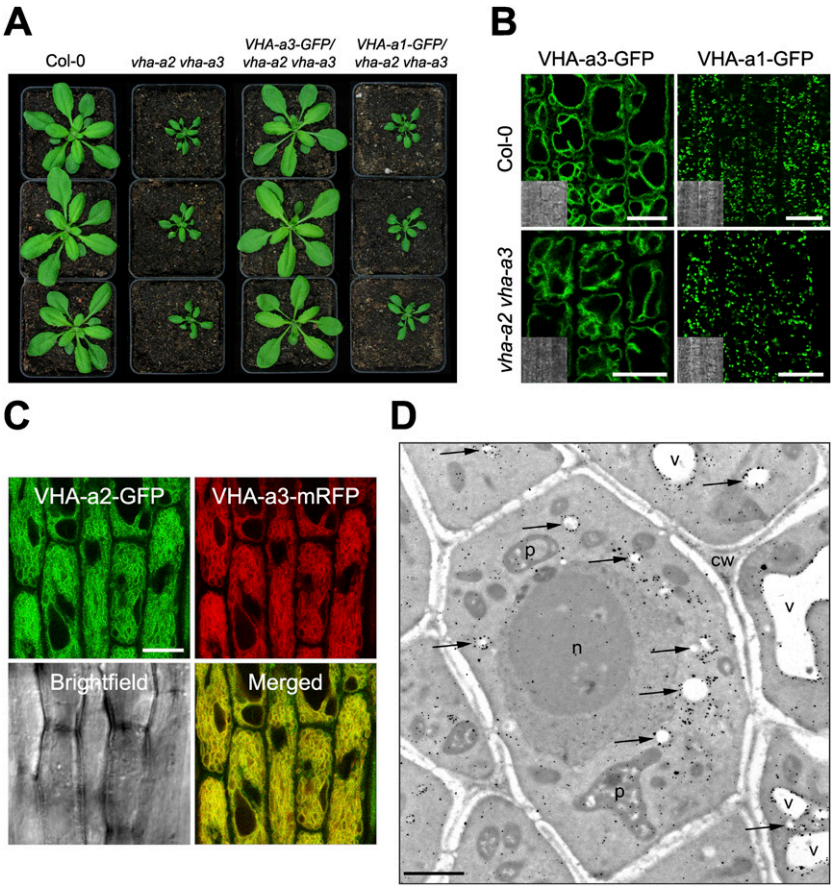

Fig. S4. VHA-a3-GFP but not VHA-a1-GFP can restore the wild-type phenotype in *vha-a2 vha-a3*. (*A*) VHA-a1-GFP and VHA-a3-GFP were stably introduced into the *vha-a2 vha-a3* mutant background. Images of soil-grown plants were taken 22 DAG. (*B*) Fluorescence images were taken within the root elongation zone of 5- to 6-day-old seedlings and illustrate the correct localization of VHA-a3-GFP and VHA-a1-GFP in the *vha-a2 vha-a3* background. (Scale bar, 20 μm.) (*C*) VHA-a2-GFP and VHA-a3-mRFP fluorescence was detected in hypocotyl hook cells of etiolated 4-day-old seedlings. Perfect colocalization at the tonoplast was obtained. Note the high density of the developing vacuolar membranes in the hypocotyl hook cells that are designated to undergo a rapid expansion. (Scale bar, 20 μm.) (*D*) Immunogold-labeled *VHA-a3-GFP* subunits in 4- to 5-day-old *Arabidopsis* root tip cells. Electron micrographs of ultrathin cryosections were labeled with anti-GFP antibodies. The tonoplast of small vacuoles (arrows) as well as of larger vacuoles is labeled. cw, cell wall; n, nucleus; p, proplastid; v, vacuole. (Scale bar, 2 μm.)

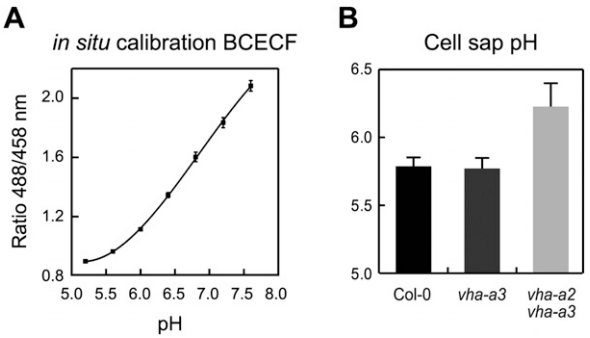

Fig. S5. pH calibration and cell sap pH. (*A*) In situ calibration was used to determine the vacuolar pH. The fluorescence ratios (488/458 nm) were plotted against the pH of the equilibration buffers to obtain a calibration curve. Error bars show SE of the mean with $n = 15$ seedlings. (*B*) In contrast to that of the wild type and the *vha-a3* mutant, the cell sap pH of *vha-a2 vha-a3* plants is more alkaline (0.44 pH units). The cell sap was measured from 3- to 4-week-old plants. Error bars show SD of three independent experiments.

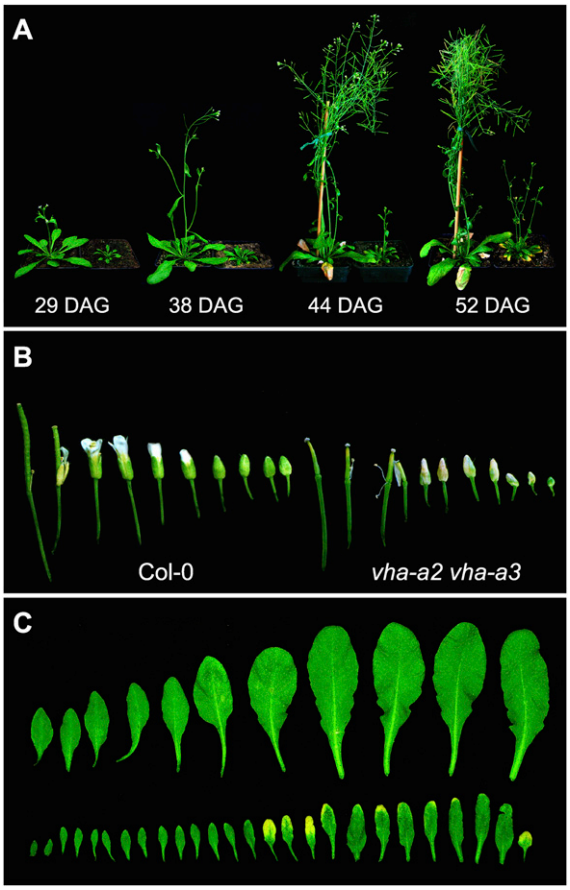

Fig. S6. Phenotype of *vha-a2 vha-a3* plants grown in soil. (*A*) *Arabidopsis* wild-type and *vha-a2 vha-a3* plants were grown in soil under 16-h light/8-h dark cycles and pictures were taken as indicated. In general *vha-a2 vha-a3* plants are delayed in growth and development. They show a reduced apical dominance and therefore appear bushier in later growth stages. (*B*) Pictures of flowers were taken 52 DAG. Mutant flowers show early senescence and under long-day conditions *vha-a2 vha-a3* fails to produce siliques. Reproduction occurs if the mutant plants are grown under continuous light. (*C*) The leaf surface (52 DAG) of *vha-a2 vha-a3* (*Lower* row) is reduced compared to that of wild type (*Upper* row). The leaf tip necrosis observed for *vha-a2 vha-a3* is indicative for nutrient deficiency.

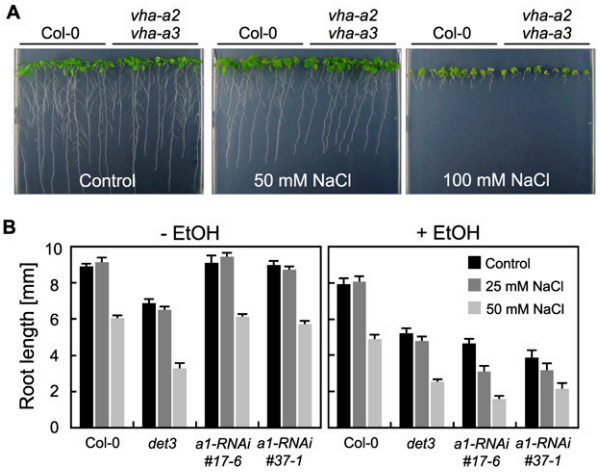

Fig. S7. Phenotype of *vha-a2 vha-a3* and *VHA-a1 RNAi* lines grown on salt. (*A*) Growth test with different salt concentrations. Seedlings were grown for 13 days under 16-h light/8-h dark cycles on vertical plates containing 1/10 MS medium, 0.5% suc, 10 mM Mes-KOH (pH 5.8), 1% agar, and the indicated concentrations of NaCl. The *vha-a2 vha-a3* mutant is not hypersensitive against NaCl. The inhibition of root growth through NaCl is similar in *vha-a2 vha-a3* and wild type. (*B*) Without induction *VHA-a1-RNAi* plants are indistinguishable from the wild type, whereas after induction with EtOH *VHA-a1 RNAi* lines became hypersensitive against NaCl treatment. Seedlings were grown for 15 days under 16-h light/8-h dark cycles on vertical agar plates with and without EtOH (0.2%) containing 1/10 MS medium, 0.5% suc, 10 mM Mes-KOH (pH 5.8), 1% agar, and the indicated concentrations of NaCl. The average root length of the seedlings was measured. Error bars represent SE of the mean with $n = 16$.